# Joint Kriging of geothermal reservoir properties – methods and challenges

Yixi Gu[1], Wolfram Rühaak[1], Kristian Bär[1] and Ingo Sass[1]

[1] Technische Universität Darmstadt, Institute of Applied Geosciences, Chair of Geothermal Science and Technology, Schnittspahnstrasse 9, D - 64287 Darmstadt, Germany

gu@geo.tu-darmstadt.de

**Keywords:** thermal conductivity, kriging with external drift, geothermal reservoir, univariate/bivariate spatial description, geostatistic modelling

## ABSTRACT

Estimating petrophysical properties of geothermal reservoirs is always a challenging task. The highest interest is typically on permeability and thermal conductivity, which are especially important parameters for numerical reservoir models. Typically only very few data exist while the budget is often small. To improve the understanding an extended and joint data exploration is therefore of vital importance.

In a pilot study the potential of extended data analysis methods is demonstrated for a Rotliegend reservoir in Germany. Along a 47 m long core measurements with a distance of only 1 mm were performed, summing up to 32,000 data points. This dense data distribution allows for studying the spatial continuity and variability in detail using one-dimensional semivariograms (spatial variance). Aim of the study is to identify spatial correlations between different physical properties, especially thermal conductivity and density, and to use this correlation for large scale volumetric estimations. Modelling variograms for mineral resource estimation is a common practice but difficult for geothermal reservoirs due to an extreme sparseness of data. To circumvent this problem the variogram is constructed on dense data sets (e.g. core and/or outcrop) and transferred into the reservoir using density values calculated based on seismic sections. The validity of this approach depends on the correlation between thermal conductivity and density. If such a correlation is given a similar spatial correlation can be presumed. Finally the volumetric calculation of the petrophysical properties can be performed by Co-Kriging or Kriging with external drift.

As an outlook the applicability of stochastic and inverse methods will be discussed.

## 1. INTRODUCTION

Within the last years, with the rapid development of renewable energies, the geothermal reservoir potential estimation became an increasingly important and challenging task. Most of the recent studies are performed to provide geophysical information (seismic, logs) and laboratory measurements as basis for geothermal modelling. For example Arndt et al. (2011) and Bär et al. (2011) modelled the 3D geothermal potential of the federal state of Hessen (Germany) using a GOCAD 3D structural model, parameterised with the statistically evaluated values of different rocks' thermophysical and hydraulic parameters (thermal conductivity, permeability, porosity and many more) using Monte Carlo methods and a multicriteria approach to evaluate the geothermal potential.

With small budgets it is vital to consider which might be the best way to deal with field observations and laboratory measurements available. All available data should be used for statistical analysis to compute best estimates and error bounds.

Kriging with external drift is a widely used technique for the spatial prediction of co-regionalized variables. Application fields in the geosciences include for example groundwater hydrogeology like Rivest et al. (2008); Kitanidis (1997) and soil sciences like Bourennane et al. (2008 and 2012) but it is only rarely used in geothermal studies.

The aims of the study are:

- to characterise the spatial variability of thermal conductivity and density
- to establish correlations of the petrophysical properties.
- to compare the result of the volumetric calculation of the petrophysical properties by different approaches.

## 2. METHOD

The core samples used in this study were collected from a research drilling "Grube Messel GA2" (GA2). It is located in the Sprendlinger Horst in the federal state of Hessen (Germany) at the coordinates of X: 3480950 and Y: 5530350 (See Fig. 1). The Permo-Carboniferous rocks are part of the sedimentation area of the largest intramontane molasse-basin of the

varsican mountains. The area of the research borehole is located between the Saar-Nahe-Basin in the west and the Werra-Fulda-Basin in the east.

The southern border of the horst is defined by mostly carboniferous intrusive crystalline bedrock of the Odenwald. In the west, the eastern fault of the Upper Rhine Graben; in the North WSW – ENE striking normal faults parallel to the river Main and in the east the Gersprenzgraben are the borders of the Horst. The whole area is characterized by fracture blocks which mostly formed during the formation of the Upper Rhine graben but show signs of reactivation of variscan faults. Two dominant strike directions exist including the conjugate faults: in the north the NE-SW fault direction is dominant; in the south the NNE-SSW fault direction is dominant. In the region of Sprendlinger Horst, the clastic and volcanic rocks of the Permo-Carboniferous cover an area of approximately 140 km² with thicknesses of up to 250 m. These Permo-Carboniferous rocks are discordantly overlain by Quaternary Eolian sands and locally by Tertiary volcanics and sediments. The underlying crystalline basement of the Sprendlinger Horst developed in the late phase of the Variscan orogenesis in the Carboniferous and is part of the Middle German Crystalline Rise.

At the end of the variscan orogenesis intramontane basins developed during the Permo-Carboniferous. The Saar-Nahe-Basin as the western part of such a basin was paleogeographically connected to the Sprendlinger Horst, which subdivided this basin from the Werra-Fulda Basin east of the Horst.

The rocks in the Saar-Nahe-Basin were deposited from Upper Carboniferous to late Permian, but in the Sprendlinger Horst, deposition only took place from the early to the late Permian.

The description of the lithology is mainly based on descriptions from similar rocks from Saar-Nahe-Basin (Schäfer 2011 and references therein) due to the little reference from the Sprendlinger Horst (Marell 1989; Müller 1996).

### 2.1 Sample Collection

In 2004, the GA2 borehole drilling was performed to investigate several Eocene deposits from the Sprendlinger Horst which were along a straight line in the east of Darmstadt and parallel to the old Variscan strike. The borehole total length is 80 m. The study only used the continuous cores from 2.5 to 50 m under the surface, which is located in the middle Moret or Langen Formation (Marell 1989) (Mainly sandstone, conglomerate, intercalated with variably fine laminated claystones). As example some core photos are presented in Fig. 2.

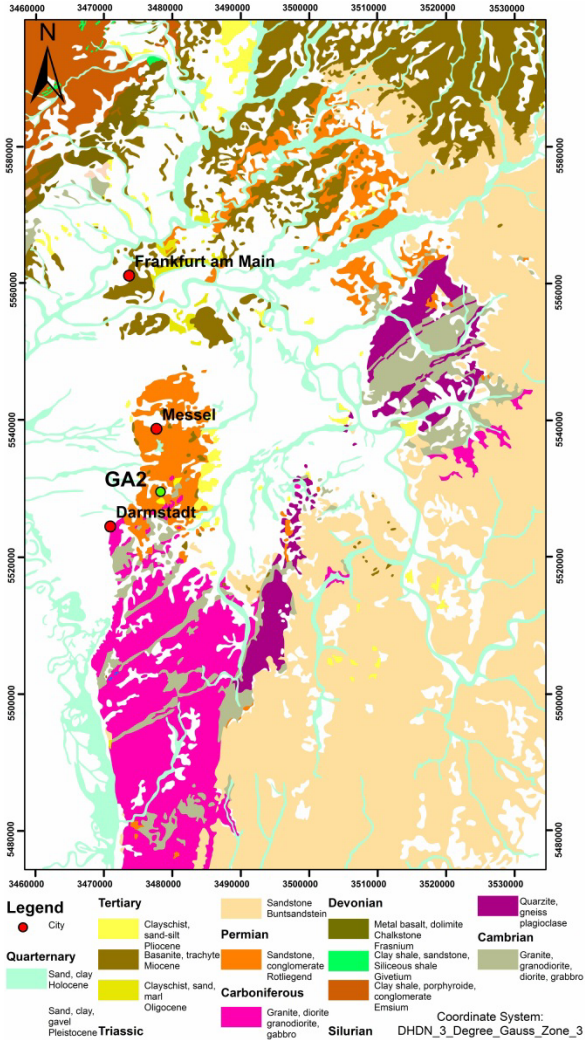


**Figure 1: Location map of Messel GA2 borehole.**

### 2.2 Laboratory Measurement

The optical scanning method (Popov et al. 1999) was employed for measuring the rock thermal conductivity both on oven dry and wet core samples due to its easy use and the possibility of continuous measurements along the whole core. The optical scanning method is based on scanning a primed and black coloured sample surface with a focused and operated mobile heat source. Along a 47 m long core measurements with a distance of only 1 mm were performed, summing up to 32,000 data points. The thermal conductivity and density profile is shown in Figure 3.

The density data used originate from the borehole geophysical logs conducted by the Leibniz Institute for Applied Geophysics (LIAG).

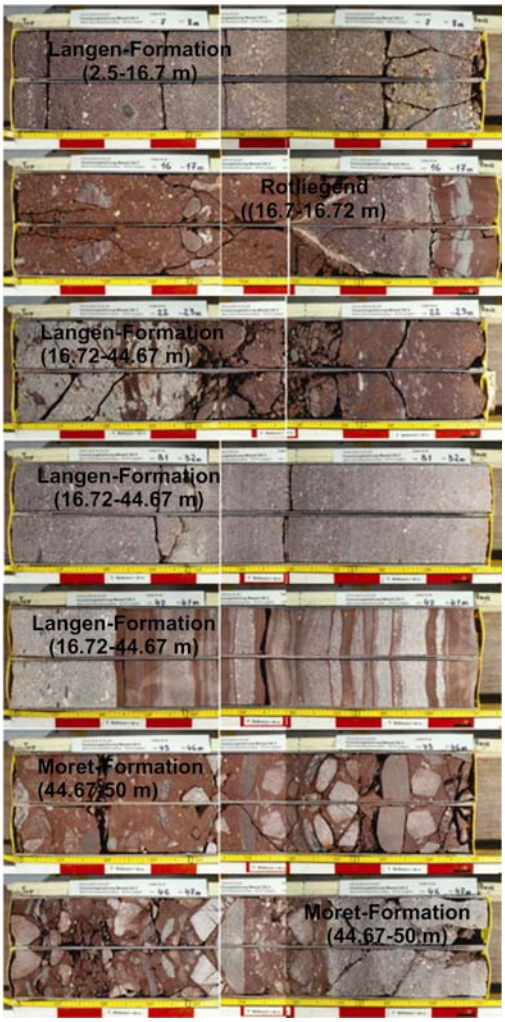


**Figure 2: Example of the core; photos are from up to down at 7-8 m, 16-17 m, 22-23 m, 31-32 m, 40-41 m, 45-46 m, and 46-47 m. The formation names are labelled on each sample as well as the distribution.**

### 2.3 Density and Thermal Conductivity Relationship

The thermal conductivity is related to the density, and within the interval 2-3 g/cm³ the density dependence for various rock types can be expressed by individual linear functions (Cermak and Rybach 1982) as Eq. 1.

$$\lambda = A + B\rho \qquad [1]$$

Where $\lambda$ is thermal conductivity; $\rho$ is the density; A and B are coefficients.

.

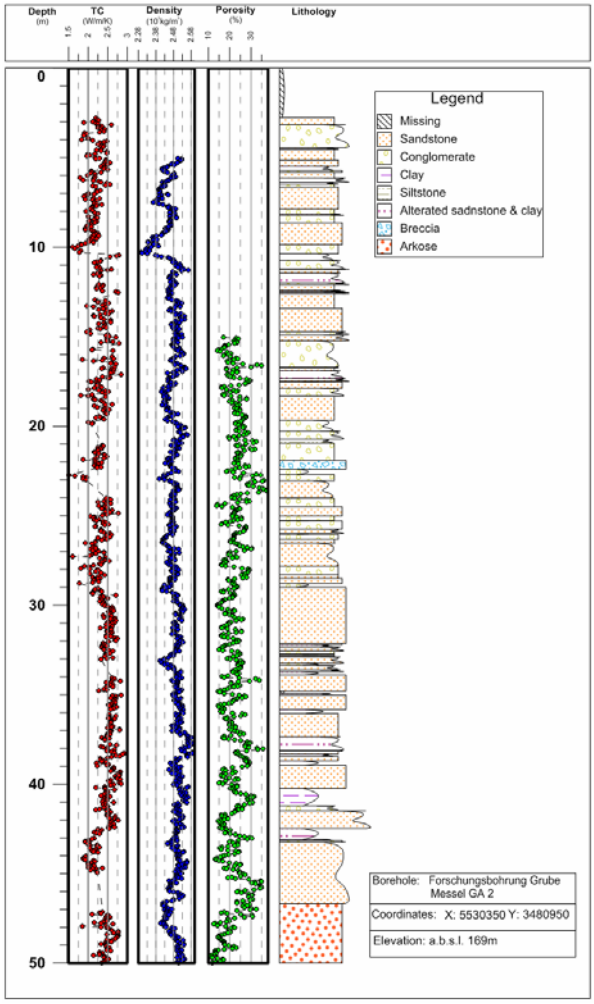


**Figure 3: Thermal conductivity (TC) and density profiles of the GA2 with lithology and porosity. The thermal conductivity.**

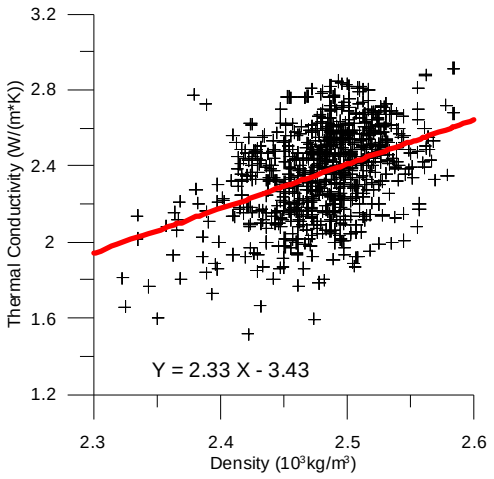


**Figure 4: Relationship diagram of all samples' thermal conductivity with density.**

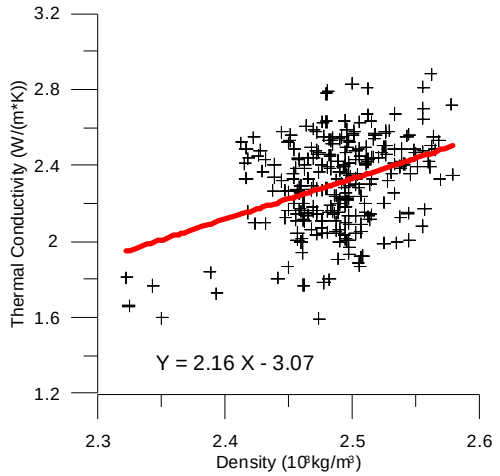


**Figure 5: Sandstone thermal conductivity versus density.**

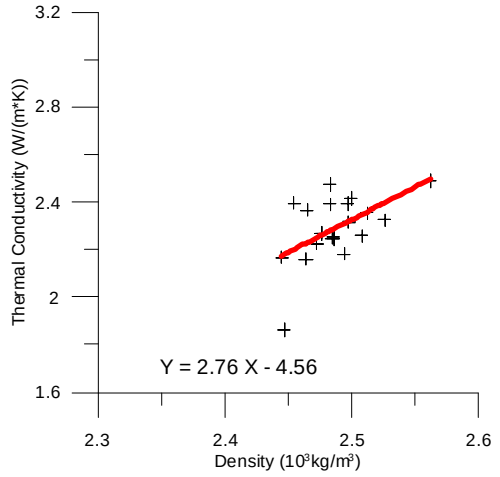


**Figure 6: Siltstone thermal conductivity versus density.**

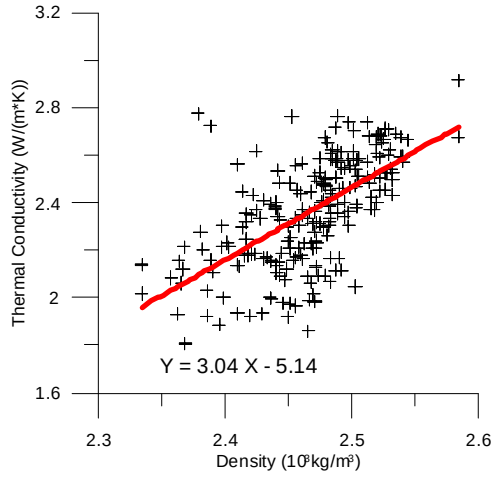


**Figure 7: Conglomerate thermal conductivity versus density.**

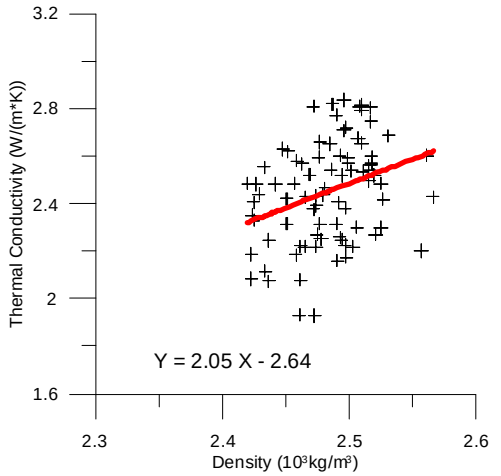


**Figure 8: Claystone thermal conductivity versus density.**

The results of the thermal conductivity measurements of the following groups: the total data (GA2), sandstone, siltstone, conglomerate and claystone are plotted in Fig. 4 to 8.

The thermal conductivity ($\lambda$) is proportional to the density ($\rho$) for most of the given series: the higher the wet bulk density the higher the thermal conductivity.

However, besides of a general correlation, i.e. increase in thermal conductivity is always somehow related to an increase of the density it becomes also obvious that the quantitative correlation is poor.

### 2.4 Variograms

Experimental variograms are a convenient tool for the analysis of spatial data as they are based on a simple measure of dissimilarity. Such a tool of geostatistical analysis is helpful to identify the spatial distribution and behaviour of the parameters studied by setting theoretical semi-variogram models that show the correlation of the variable in different directions and distances of separation. These models can estimate the values of the studied variable in areas not sampled by interpolation through ordinary kriging (Dale et al. 2002).

The variability of a regionalized variable $Z(x)$ is measured along the core depth by calculating the dissimilarity between pairs of data values, $Z_1$ and $Z_2$ for example, located at two points $x_1$ and $x_2$ in the core.

The dissimilarity $\gamma$ depends on the spacing and on the orientation of the point pair, which is described by a vector $h = x_2 - x_1$,

$$\gamma(h) = \frac{1}{2}[(Z(x+h) - Z(x))^2] \quad [2]$$

By forming the average of the dissimilarities $\gamma(\Delta x)$ for all $N_h$ point pairs that can be linked by a vector $h$, we obtain the experimental variogram.

$$\gamma(h) = \frac{1}{2N_h}\sum_{\alpha=1}^{N_h}[(Z(x_\alpha + h) - Z(x_\alpha))^2] \qquad [3]$$

Usually it can be observed that the dissimilarity between values increases on average when the spacing between the pairs of sample points is increased at low separation distance.

The variogram can be discontinuous at the origin, due to the ‘’nugget-effect’’, which means that the values of the variable change abruptly at a very small scale, like gold grades when a few gold nuggets are contained in the samples (Hudson and Wackernagel 1994).

For the measured thermal conductivity values a theoretical variogram was estimated with no nugget effect. A spherical model was fitted to the variogram and this model (see Fig. 9) is used in Ordinary Kriging (OK) and Kriging with External Drift (KED) (Chauvet and Galli 1982).

**Table 1 Summary statistics for measured dry thermal conductivity.**

| | |
|---|---|
| Minimum | 1.107 |
| Maximum | 3.745 |
| Mean | 2.3638 |
| Median | 2.3900 |
| Standard deviation | 0.2670 |
| Variance | 0.071 |
| Skewness | -0.379 |
| Kurtosis | 0.469 |
| Number of observations | 31049 |

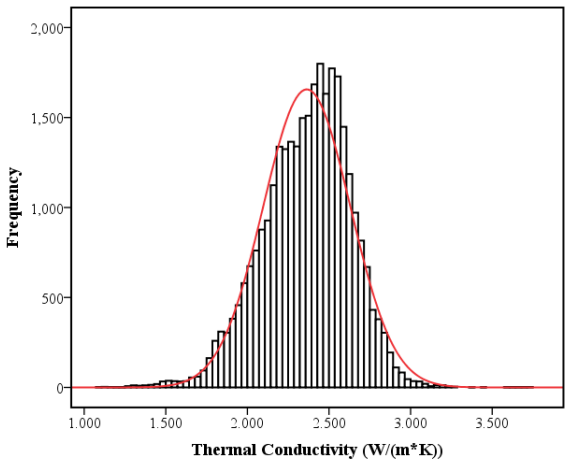


**Figure 9 Histogram of measured thermal conductivity. The red solid line shows normal distribution.**

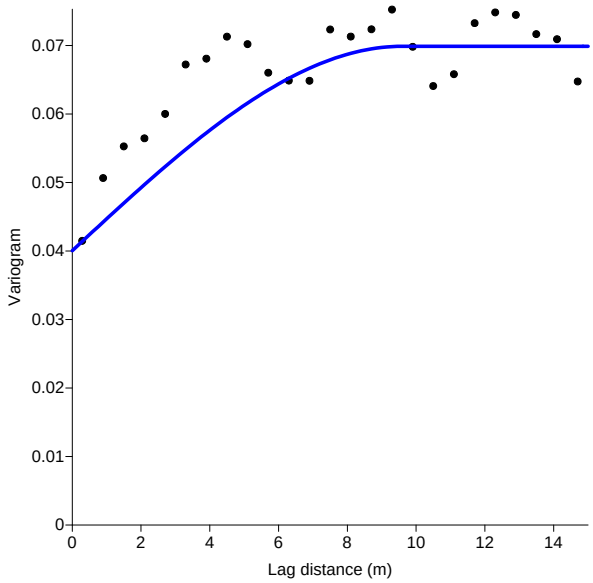


**Figure 10 Variograms of thermal conductivity fitted with a spherical and a nugget model fitted to lag 15 m. The nugget effect is 0.04, sill is 0.03 and range is 9.59 m.**

## 2. Ordinary kriging theory

When the local mean may vary significantly over the study area, for example, the thermal conductivity of 9.7 – 10 m varies from 1.416 to 2.013 W/(m*K), depending on the low density; recall that the overall thermal conductivity is 2.364 W/(m*K).

Ordinary kriging (OK) allows one to account for such local variation of the mean by limiting the domain of stationarity of the mean to the local neighbourhood $W(u)$ centered on the location $u$ being estimated.

$$Z^*(u) - m(u) = \sum_{\alpha=1}^{n}\lambda_\alpha(u)[Z(u_\alpha) - m(u_\alpha)] \qquad [4]$$

where $Z^*(u)$ is the variants of the basic linear regression estimator. $\lambda_\alpha(u)$ is the weight assigned to datum $z(u_\alpha)$ interpreted as a realization of the $RV\ Z(u_\alpha)$. The quantities $m(u)$ and $m(u_\alpha)$ are the expected cvalues of the $RVs\ Z(u)$ and $Z(u_\alpha)$. The

number of data involved in the estimation as well as their weights may change from one location to another.

The linear estimator [4] is then a linear combination of the $n(u)$ RVs $Z(u_\alpha)$ plus the constant local mean $m(u)$:

$$Z^*(u) = \sum_{\alpha=1}^{n(u)} \lambda_\alpha(u) Z(u_\alpha) + \left[1 - \sum_{\alpha=1}^{n(u)} \lambda_\alpha(u)\right] m(u) \quad [5]$$

The unknown local mean $m(u)$ is filtered from the linear estimator by forcing the kriging weights to sum to 1. The ordinary kriging estimator $Z^*_{OK}(u)$ is thus written as a linear combination only of the $n(u)$ RVs $Z(u_\alpha)$:

$$Z^*_{OK}(u) = \sum_{\alpha=1}^{n(u)} \lambda_\alpha^{OK}(u) Z(u_\alpha)$$

$$\text{with } \sum_{\alpha=1}^{n(u)} \lambda_\alpha^{OK}(u) = 1 \quad [6]$$

The OK estimator [6] is unbiased since the error mean is equal to zero.

The minimization of the error variance under the non-bias condition $\sum_{\alpha=1}^{n(u)} \lambda_\alpha^{OK}(u) = 1$ calls for the definition of a Lagrangian $L(u)$, which is a function of the data weights $\lambda_\alpha^{OK}(u)$, and a Lagrange parameter $2\mu_{OK}(u)$:

$$L\left(\lambda_\alpha^{OK}(u), \alpha = 1, \dots, n(u); 2\mu_{OK}(u)\right) = \sigma_E^2(u) + 2\mu_{OK}(u)\left[\sum_{\alpha=1}^{n(u)} \lambda_\alpha^{OK}(u) - 1\right] \quad [7]$$

The optimal weights $\lambda_\alpha^{OK}(u)$ are obtained by setting to zero each of the $(n(u) + 1)$ partial first derivatives:

$$\frac{1}{2}\frac{\partial L(u)}{\partial \lambda_\alpha^{OK}(u)} = \sum_{\beta=1}^{n(u)} \lambda_\beta^{OK}(u) C_R(u_\alpha - u_\beta) - C_R(u_\alpha - u) + \mu_{OK}(u) = 0 \quad (\alpha = 1, \dots, n(u))$$

$$\frac{1}{2}\frac{\partial L(u)}{\partial \mu_{OK}(u)} = \sum_{\alpha=1}^{n(u)} \lambda_\alpha^{OK}(u) - 1 = 0$$

The ordinary kriging system includes $(n(u) + 1)$ linear equations with $(n(u) + 1))$ unknowns: the $(n(u)$ weights $\lambda_\alpha^{OK}(u)$ and the Lagrange parameter $\mu_{OK}(u)$ that accounts for the constraint on the weights:

$$\begin{cases} \sum_{\beta=1}^{n(u)} \lambda_\beta^{OK}(u) C_R(u_\alpha - u_\beta) + \mu_{OK}(u) = C_R(u_\alpha - u) \\ \qquad \alpha = 1, \dots, n(u) \\ \sum_{\beta=1}^{n(u)} \lambda_\beta^{OK}(u) = 1 \end{cases} \quad [8]$$

Although the mean $m(u)$ is assumed stationary only with the local neighbourhood $W(u)$, leading to the following system:

$$\begin{cases} \sum_{\beta=1}^{n(u)} \lambda_\beta^{OK}(u) C(u_\alpha - u_\beta) + \mu_{OK}(u) = C(u_\alpha - u) \\ \qquad \alpha = 1, \dots, n(u) \\ \sum_{\beta=1}^{n(u)} \lambda_\beta^{OK}(u) = 1 \end{cases} \quad [9]$$

The resulting minimum error variance, called OK variance, is obtained by substituting the first $n(u)$ equations of the ordinary kriging system [9] into the error variance (Goovaerts, 1997):

$$\sigma_{OK}^2(u) = C(0) - \sum_{\beta=1}^{n(u)} \lambda_\beta^{OK}(u) C(u_\alpha - u) - \mu_{OK}(u) \quad [10]$$

### 2.5 Kriging with a trend model theory

The mean function $m(u)$ is called the 'drift'. The KT estimator of the trend is expressed as a linear combination of $n(u)$ random variables:

$$m^*_{KT}(u) = \sum_{\alpha=1}^{n(u)} \lambda_\alpha^{KT} m(u) Z(u_\alpha) \quad [11]$$

where $\lambda_\alpha^{KT} m(u)$ is the weight.

The $(K + 1)$ unknown coefficients $a_k(u)$ are filtered from the linear estimator by imposing the following $(K + 1)$ constraints:

$$\sum_{\alpha=1}^{n(u)} \lambda_\alpha(u) f_k(u_\alpha) = f_k(u) \quad k = 0, \dots, K \quad [12]$$

By convention, the first trend function $f_0(u)$ is the unit constant, that is $f_0(u) = 1$. Hence the first condition is similar to the OK constraint on the weights: $\sum_{\alpha=1}^{n(u)} \lambda_\alpha(u) = 1$.

The constraints allow one to express the KT estimator as linear combination of only the $n(u)$ RVs $Z(u_\alpha)$:

$$Z^*_{KT}(u) = \sum_{\alpha=1}^{n(u)} \lambda_\alpha^{KT}(u) Z(u_\alpha) \quad [13]$$

with $\sum_{\alpha=1}^{n(u)} \lambda_\alpha^{KT}(u) f_k(u_\alpha) = f_k(u)$ $k = 1, \dots, K$

The kriging with trend estimator is unbiased since the error mean is equal to zero:

$$E\{Z^*_{KT}(u) - Z(u)\} = \sum_{\alpha=1}^{n(u)} \lambda_\alpha^{KT}(u) m(u_\alpha) - m(u) = 0$$

The minimization of the corresponding error variance, under the $(K + 1)$ non-bias conditions calls for the definition of a Lagrangian $L(u)$. The procedure is similar to that for ordinary kriging except that there are now $(K + 1)$ Lagrange parameters $\mu_k^{KT}(u)$ accounting for the $(K + 1)$ constraints on the weights.

Setting the $(n(u) + K + 1)$ partial first derivatives to zero yields the following system of $(n(u) + K + 1)$ linear equations:

$$\begin{cases} \sum_{\beta=1}^{n(u)} \lambda_\beta^{KT}(u) C_R(u_\alpha - u_\beta) + \sum_{k=0}^{K} \mu_k^{KT}(u) f_k(u_\alpha) = C_R(u_\alpha - u) & \alpha = 1, \dots, n(u) \\ \sum_{\beta=1}^{n(u)} \lambda_\beta^{KT}(u) = 1 & \\ \sum_{\beta=1}^{n(u)} \lambda_\beta^{KT}(u) f_k(u_\beta) = f_k(u) & k = 1, \dots, K \end{cases} \quad [14]$$

Accounting for the first $n(u)$ equations in system [14], the minimized error variance becomes

$$\sigma_{KT}^2(u) = C_R(0) - \sum_{\alpha=1}^{n(u)} \lambda_\alpha^{KT}(u) C_R(u_\alpha - u) - \sum_{k=0}^{K} \mu_k^{KT}(u) f_k(u) \quad [15]$$

Note that for $K = 0$, system [14] reverts to the ordinary kriging system [8]. Thus, the KT estimator [13] and kriging variance [15] are equal to the OK estimator [6] and kriging variance [10].

Kriging with a trend model requires a prior determination of (1) the K trend functions $f_k(u)$, and (2) the covariance of the residual component $R(u)$, $C_R(h)$ (Goovaerts 1997).

The auxiliary variables should be incorporated in the form of an external drift only if they are highly linearly correlated with the variable of interest. Otherwise it is preferable to use the method of co-kriging, which requires the fitting of a model for the cross-variograms between the different variables (Hudson and Wackernagel 1994).

With the significant linear relation exists between thermal conductivity and density, it is possible to fit a variogram in 1D (only depth) and use density as an internal drift.

The two estimators differ by the definition of the trend component. Figure 10 shows both KED (solid red line) and OK (dashed blue line) estimates of the variables of transformed thermal conductivity. Both KED and OK estimates are fairly similar. The largest differences occur for the missing value segment (like underground 44 to 48 meter), where the two KED and OK slope estimates differ more. The secondary parameter contribution influences the estimates in the Kriging with an external drift.

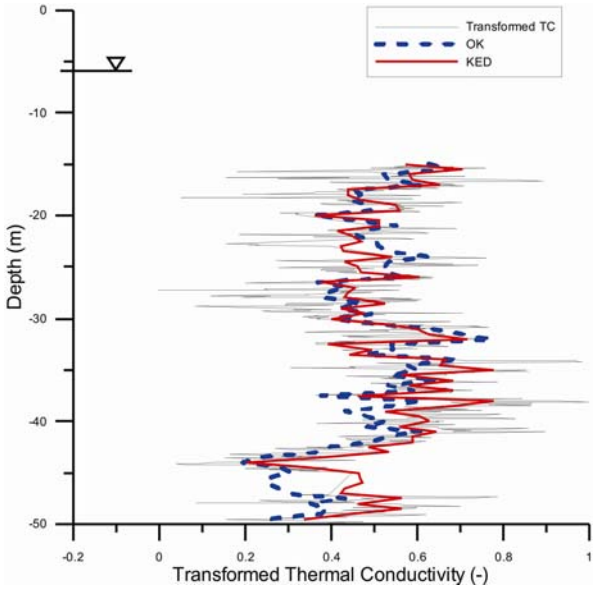


**Figure 10 Kriging thermal conductivity (TC) with density drift. The gray line is transformed thermal conductivity. The dashed blue line and the solid red line indicate respectively the results of Ordinary Kriging and Kriging with External Drift (KED).**

## 3. CONCLUSIONS

Ordinary kriging as well as KED are established on the basis of the variogram function which represents the spatial data variability.

These first tests show the principal applicability of multi-variable geostatistics for improving the forecast of reservoir parameters. Future work will be to test advantages of Co-Kriging compared to KED. Once these tests are completed the geostatistical approach will be applied to a large seismic data-set which is available at the borehole location. Here seismic data, which are also strongly correlated with density, will be used for derivation of a large scale variogram and will be used as secondary variable while interpolating the density.

## REFERENCES

Armstrong, M.: Problems with universal kriging, Math. Geol., 16, (1984), 101-108.

Arndt, D., Baer, K., Fritsche, J.-G., Kracht, M., SASS, I. and HOPPE, A.: 3D structural model of the Federal State of Hesse (Germany) for geo-potential evaluation, *Z. dt.Ges. Geowiss*., 162 (4), Stuttgart, (2011), 353-370.

Bär, K., Arndt, D., Fritsche, J-.G., Götz, A. E., Kracht, M. Hoppe, A and Sass, I.: 3D-Modellierung der tiefengeothermischen Potenziale von Hessen, – Eingangsdaten und Potenzialausweisung, *Z. dt.Ges. Geowiss.* , (2011), 162/4, 371-388.

Bourennane, H., King, D. and Couturier, A.: Comparison of kriging with external drift and

simple linear regression for predicting soil horizon thickness with different sample densities, Geoderma, 97, (2008), 255–271.

Bourennanea, H., Nicoullauda B., Couturiera A., Pasquiera C., Maryb, B, and Kinga, D.: Geostatistical filtering for improved soil water content estimation from electrical resistivity data, Geoderma, 183–184, (2012), 32–40.

Cermak, V. and Rybach L.: Thermal conductivity and specific heat of minerals and rocks, in: landolt-Börnstein: Numerical data and fuctional relationship in Science and technology, Angenheister, G. (Ed.), 305-343, Springer, Berlin-Heidelberg, (1982).

Chauvet, P. and Galli, A.: Universal Kriging. Publication C-96, Centre de Mines de Geostatistique, Ecole des Mines de Paris, Fontainebleau, (1982), 94.

Dale, M., Dixon, P., Fortin, M., Legendre, P., Myers, D. and Rosemberg, M: Conceptual and mathematical relationships among methods for spatial analysis, Ecography, 25, (2002), 558-77.

Goovaerts, P.: Geostatistics for Natural Resources Evaluation, Oxford university press, New York, (1997).

Hudson, G. and Wackernagel, H: Mapping temperature using kriging with external drift: theory and an example from Scotland, International Journal of Climatology, 14, (1994), 77–91.

Kitanidis, P.K.: Introduction to Geostatistics An Introduction to Applied Geostatistics, Oxford University Press, New York, (1997).

Popov, Y.A., Pribnow, D.F.C., Sass, J.H.; Williams, C.F.; Burkhardt, H.: Charaterization of rock thermal conductivity by high-resolution optical scanning, Geothermics, 28, 2, (1999), 253-276.

Marell, D.: Das Rotligend zwischen Odenwald und Taunus, Geologsiche Abhandlungen Hessen, Hessiches landesamt für Bodenforschung, Wiesbaden, (1989), 89, 128.

Müller, H.: Das Permokarbon im nördlichen Oberrheingraben – Paläogeographische und strukturelle Entwicklung des permokarbonen Saar-Nahe-Beckens im nördlichen Oberrheingraben,(1996), *Geol. Abh. Hessen*, 99, 85 S., Wiesbaden.

Rivesta, M., Marcottea, D. and Pasquierb, P.: Hydraulic head field estimation using kriging with an external drift: A way to consider conceptual model information, 361, (2008), 349–361.

Razack, M. and Lasm, T.: Geostatistical estimation of the transmissivity in a highly fractured metamorphic and crystalline aquifer (Man-Danane Region, Western Ivory Coast), Journal of Hydrology, 325, (2006), 164–178.

Schäfer, A.: Tectonics and sedimentation in the continental strike-slip Saar-Nahe Basin (Carboniferous, West Germany). [Tektonik und Sedimentation im kontinentalen Saar-Nahe-Becken (“Strike-slip”-Modell, Karbon-Perm, Westdeutschland).], (2011), *Z. dt. Ges. Geowiss*., 162, 127-155, Stuttgart.

**Acknowledgements**

The authors are grateful for access to the drill cores and the borehole geophysical data by courtesy of the Leibniz Institute for Applied Geophysics (LIAG) and the Forschungsinstitut Senckenberg, Grube Messel.